

800kV 가스차단기의 아크특성 해석

V.V. Chulkov*, 신영준, 박경엽, 송기동, 최영길
 한국전기연구소 개폐장치연구팀, * V.E.I Russia

The numerical analysis of gas blast arcs for 800kV GCB

V.V. Chulkov*, Y.J. Shin, K.Y. Park, K.D.Song, Y.K.Choi
 KERI Switchgear Research Team, *V.E.I Russia

Abstract

For the analysis of hot gas flow due to arc in puffer type SF₆ gas circuit breakers(GCBs), a program has been developed by adding function for arcing to the Fluid-in-Cells(FLIC) method, which is often used for a two dimensional compressible flow problems, utilizing a simplified enthalpy flow arc model available for arcing. In this paper, the results of arc modelling for 800kV GCB are presented and compared with that of cold gas flow in the interrupters. It is shown that the nozzle clogging is the dominating factor in the pressure rise of the puffer chamber. It permits to estimate the dielectric strength of interrupters.

1. Introduction

In modern gas-blast switchgear, the arc plays a critical role in controlling nozzle clogging and pressure rise. The increasing arc current leads to the increasing pressure in the puffer cylinder of circuit interrupters, when the arc diameter reaches that of the nozzle throat or beyond it, the ablated nozzle material generates reversal flow towards the high pressure side of nozzle, up to the cylinder. For getting good dielectric recovery characteristics of the interrupter, it is strongly needed to develop a suitable arc model which allows to predict the behavior of gas flow.

An arc burning in a nozzle is very similar to a round jet where the most part of the input power is carried off by internal supersonic flow. The objective of this investigation is to apply a simplified enthalpy flow arc model to the gas dynamic problems in SF₆ circuit breakers.

A comprehensive understanding of this type of arcs is of interest for modern power circuit breakers.

Two zones are presented to model the gas flow caused by arc. The one is the arc zone in which the mass flow is negligibly small. The arcs can be considered as a solid body when compared with the surrounding gas. For arc zone, the enthalpy flow model is used [1]. The influence of the arc radiation on the heating gas is taken into account. At this time, the data for net emission coefficient and fraction of radiation is adopted from [2]

2. Governing equations and numerical simulation model

Basic equations for an axisymmetric compressible gas flow are expressed as follows:

$$\frac{\partial \vec{F}}{\partial t} + \nabla \vec{F} \cdot \vec{v} = \vec{J}$$

where $\rho = \rho(P, T)$

$$\vec{F} = \begin{bmatrix} \rho \\ \rho u \\ \rho v \\ \rho e \end{bmatrix}, \quad \vec{J} = \begin{bmatrix} 0 \\ \frac{\partial P}{\partial r} \\ \frac{\partial P}{\partial z} \\ \frac{\partial P \cdot u}{\partial r} + \frac{\partial P \cdot v}{\partial z} + P_{in} \end{bmatrix}$$

In the above equations u and v are respectively the radial and axial component of the velocity vector \vec{v} ,

P : pressure, c_v : specific heat capacity, ρ : the mass density, e : specific total energy ($e = c_v \cdot T + \frac{(u^2 + v^2)}{2}$)

, P_{in} : an input power and T : temperature.

The input power is calculated as follows :

i) For arc zone, This is jole heating

$$P_{in} = J^2 / \sigma$$

ii) For cold gas area, this is radiation absorbtion

$$P_{in} = r_d^2 \frac{U}{r^2} \frac{e^{-r/r_{ab}}}{r_{ab}}$$

where J : current density, σ : electrical conductivity, U : radiation power per unit arc length, r_{ab} : absorbtion length, r_d : arc radius. The thermodynamic properties are functions of temperature and pressure, which can be taken from [1].

To save calculating time the modeling area is limited to nozzle and arc area. The calculation areas are connected to two tanks. One is the puffer cylinder where the gas is compressed with the piston movement. Another is a downstream area connected to nozzle. The mass flows between these areas are treated as the quasistationary adiabatic approximation.

The mass flow through cross section A is given by

$$\dot{m} = A \left[\frac{P_d}{P_u} \right]^{\frac{1}{\gamma}} \left[\frac{2\gamma}{(\gamma-1)} \rho_u P_u \left(1 - \left[\frac{P_d}{P_u} \right]^{\frac{\gamma-1}{\gamma}} \right) \right]^{\frac{\gamma-1}{\gamma}}$$

where P_u : the pressure of upstream, P_d : the pressure of downstream, ρ_u : gas density of upstream, γ : adiabatic coefficient of the gas. In the puffer cylinder, the compression is considered as adiabatic condition.

The equations for mass and energy are

$$V \frac{d\rho_u}{dt} = -\dot{m} + \rho_u A u_c$$

$$\frac{d(Ve\rho_u)}{dt} = -\dot{m}e + P_u A u_c$$

$$P_u = e\rho_u(\gamma - 1)$$

where u_c : piston velocity, V : volume of the puffer cylinder.

The fluid in cell (FLIC) method [3,4] is used to solve the governing equation. Even with nonuniform grid, [52 × 120] cells are required to obtain sufficiently accurate solution. The time marching technique is used for the calculations starting from the initial position of the piston and the moving contacts. At this time the uniform

distributions of gas density, pressure and temperature are assumed. The time step is chosen from the Courant-Friedrichs-Lewy condition.

3. Result and discussion

The gas density, pressure, velocity and temperature are obtained from calculation along the stroke curve. Fig. 1 shows the typical velocity distributions for 800 kV model interrupter at few times with 40kA arc. It is necessary to make few remarks with reference to the arc influence on the gas flow. The gas flow can be interrupted because of lack of flow passage. This clogging phenomena creates the gas pressure rise in cylinder area. Fig.2 shows pressure rise in puffer cylinder for two cases, hot and cold(without arc) gas flows. A considerable gap between these two cases is shown. The stagnation point pressure of the case of the hot gas flows is presented too. Little difference between the pressure of the puffer cylinder and the stagnation point pressure is indicated.

The dielectric recovery capability can be derived from calculations. The electrical breakdown voltage is proportional to the gas density. So it is possible to make an estimate of the breakdown voltage from this numerical simulations. The typical gas density distribution at current zero time is shown in Fig.3. The considerable decrease of gas density near stationary contact is shown.

The thermal breakdown capability (the rate of rise of recovery voltage(r.r.r.v) at current zero) can also be estimated by using our stagnation point pressure of the calculation and Frind and Rich results [5], where the experimental dependences of r.r.r.v on pressure and current are presented. Resently, the arc modeling at current zero time has been developed for r.r.r.v estimate.

Therefore, this model can be used as initial condition for current zero problem.

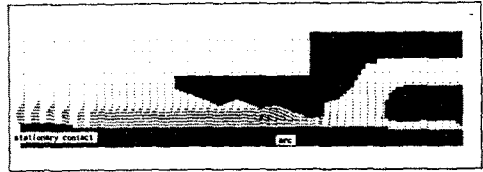
4. Conclusion

Our principal results relate to the gas dynamic flow in SF₆ circuit breakers. The arc model presented allows systematical quantification of the puffer type gas circuit breaker design. The distributions of the gas density, velocity, pressure are obtained as a time fuction for 800kV

GCB. The arc behavior and its influence on gas flow have been investigated in details. It is shown that the considerable rise of the gas pressure in the puffer cylinder is caused by the phenomena of the nozzle clogging.

References

1. L.S.Frost and R.W.Liebermann Composition and transport properties of Sf_6 and their use in a simplified enthalpy flow arc model Proc IEEE, v. 59, p. 474-485, 1971
2. R.W.Liebermann and J.J.Lowke Radiation emission coefficient for sulfur hexafluoride arc plasmas JQSRT v.16, p299-327, 1975
3. R.A.Gentry, R.E.Martin and B.J.Daly An Eulerian differencing method for unsteady compressible flow problems J. Comp. Phys. v. 1, p. 87-118, 1966
4. O.M.Belotzerkovsky, Y.M.Davydov Unsteady particle in cell method for gas dynamic problems J comp.math. and math. phys. (Sov.Union), v.11, p.182-207,1971
5. G.Frind and J.A.Rich Recovery speed of axial flow gas blast interrupter: dependence on pressure and di/dt for air and SF_6 IEEE Trans. Power App. Syst v.93, p.1675-1684, 1974



(d) Gas velocity distribution at 31ms

Fig 1. Typical velocity distributions for 800kV GCB

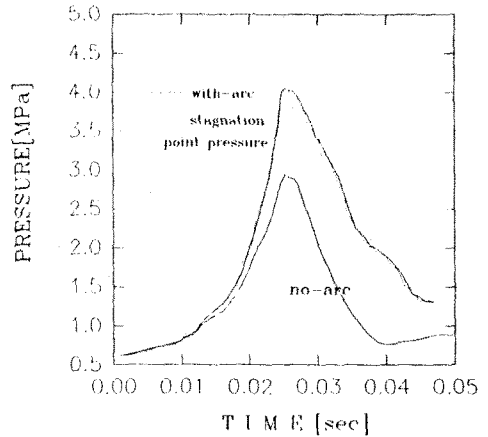
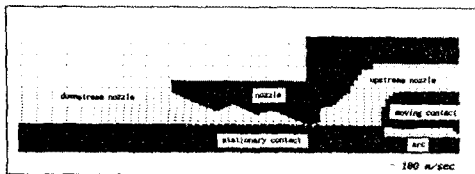
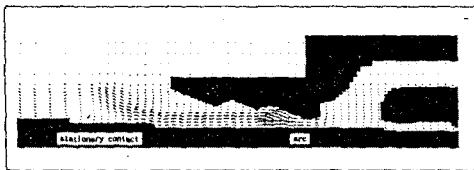


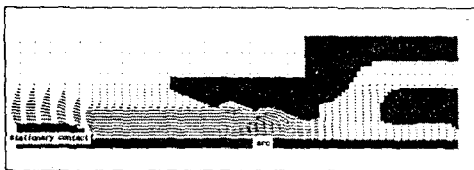
Fig 2. Pressures in the puffer cylinder of 800kV GCB and stagnation point pressure



(a) Gas velocity distribution at 14ms



(b) Gas velocity distribution at 20ms



(c) Gas velocity distribution at 25.5ms

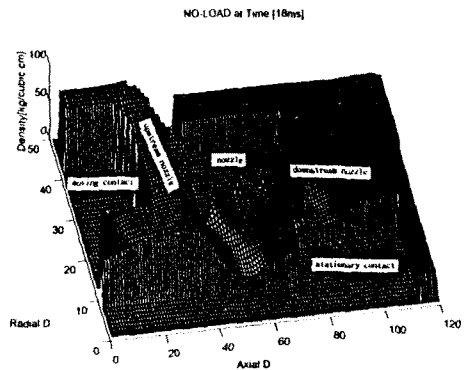


Fig 3. Typical gas density distribution at current zero time